JOURNAL OF CATALYSIS 101, 19–27 (1986)

# Characterization of Organically Pillared Zirconium Phosphates

BEN-ZU WAN,* RAYFORD G. ANTHONY,* GUANG ZHI PENG,† AND ABRAHAM CLEARFIELD†

*Kinetics, Catalysis and Reaction Engineering Laboratory Department of Chemical Engineering; and †Department of Chemistry, Texas A&M University, College Station, Texas 77843

Received November 26, 1985; revised March 20, 1986

Samples of α-zirconium phosphates and of zirconium phosphates pillared by phenyl, dimethylphenyl, and diphenyl have been characterized by BET surface area, surface acidity, adsorption capacity and pore sizes, TGA, X-ray powder diffraction, and activity for isopropanol decomposition. The BET surface areas of pillared zirconium phosphates have been found to increase with the increase in size and number of organic groups in the interlayers. The total number of surface acidic sites of α-zirconium phosphates has been found to be greater than any one of the pillared catalysts. It is concluded from this study that α-zirconium phosphate pillared by diphenyl has interlayer openings large enough to sorb isopropanol, and its decomposition takes place mainly in the interlayers of this catalyst. In contrast, the phenyl and dimethylphenyl pillared zirconium phosphates have less free space between the interlayers so that the reactions of isopropanol take place on the outer surface of the catalysts. The dehydration of isopropanol to propylene has been found to be the primary reaction for all the catalysts. 

## INTRODUCTION

The use of α-zirconium phosphates as catalysts in several reactions, viz., dehydration of cyclohexanol (*1*), dehydrogenation of cyclohexene (*2*), ethylene oxidation (*3*), and methanol conversion (*4*), has received considerable attention. Although zirconium phosphates have layered structures, the intracrystalline pore size is small and allows reactions to occur only on the surface and not in the interior of the crystals (*5, 6*). Recently, it was shown that α-zirconium phosphates could be pillared by organic phosphates and phosphonates (*7*), thereby increasing the interlayer distance, pore size, and surface area. Dines *et al.* (*7*) have presented idealized structures and *d*-spacings for these pillared materials. In this paper, we present the characterization of some of these organically pillared zirconium phosphates by TGA, X-ray diffraction powder patterns, pore volume and pore size, BET surface area, temperature-programmed desorption (TPD) of ammonia, and isopropanol decomposition. The catalysts studied were a semicrystalline α-zirconium phosphate, $Zr(HPO_4)_2$, designated α-ZrP, and zirconium phosphate phosphonates in which the organic groups bridged across the layers.

## EXPERIMENTAL

*Catalyst preparation.* Five samples were prepared, four were of the mixed component-pillared type, $Zr(HPO_4)_{2-2x}(O_3P\text{-}R\text{-}PO_3)_x$, and one was a normal layered α-zirconium phosphate (*6*). The latter sample was prepared by refluxing a zirconium phosphate gel in 2.5 *M* $H_3PO_4$ for 48 h. This procedure has previously been shown to lead to a semicrystalline product of composition, $Zr(HPO_4)_2 \cdot H_2O$, and a surface area of about 30 $m^2/g$ (*8*). The organically pillared derivatives were prepared from the corresponding diphosphonic acid–$H_3PO_4$ mixtures and zirconyl chloride as described by Dines *et al.* (*9, 10*). In order to achieve greater crystallinity, the preparations were carried out in the presence of HF. The HF complexes the zirconium and releases it slowly during the reaction. The conditions



0021-9517/86 $3.00

TABLE 1

Preparative Conditions and Analytical Results for Catalyst Samples

| Sample No. | Formula | Preparative condition | | %Carbon | | %Hydrogen | | LOI[c] (%) |
|---|---|---|---|---|---|---|---|---|
| | | HF/Zr | $H_3PO_4$/ORG[b] | Obs | Calcd | Obs | Calcd | |
| α-ZrP (2.5 : 48) | $Zr(HPO_4)_2 \cdot H_2O$ | 0 | ∞ | — | — | — | — | 12.0 |
| P-1-7-7 | $Zr(HPO_4)_{0.74}(O_3P\phi^{a}\ PO_3)_{0.63}$ | 13 | 4 | 14.2 | 14.6 | 1.36 | 1.06 | — |
| MPM-6-1 | $Zr(HPO_4)_{0.88}(O_3PCH_2\ \phi CH_2 - PO_3)_{0.56}$ $2.7H_2O$ | — | — | 14.49 | 14.49 | 2.30 | 2.9 | 33.58 |
| PP-2-5-1 | $Zr(HPO_4)_{0.17}(O_3P\phi\phi PO_3)_{0.914}$ $0.638(H_2PO_4\phi\phi PO_4H_2)1.9H_2O$ | 18 | 6 | 40.11 | 35.5 | 2.49 | 3.05 | 59.5 |
| PP-2-5-12 | $Zr(HPO_4)_{0.764}(O_3P\phi\phi PO_3)_{0.618}1.59H_2O$ | 10 | 2 | 23.5 | 23.1 | 2.3 | 2.3 | 41.06 |

[a] $\phi$ represents phenyl group.
[b] Organophosphonate.
[c] Loss on ignition.

of preparation and results are presented in Table 1. All the organically pillared preparations were carried out at 60–70°C for 3–7 days.

*BET surface area and adsorption experiments.* These experiments were performed on a Micromeritics Accusorb 2100E unit. The samples were degassed at 200°C under high vacuum ($10^{-5}$–$10^{-6}$ Torr) overnight. The procedures published by Micromeritics were used for the measurement of surface area and of the adsorption isotherm.

*Measurement of acid sites.* The acidity and acidic sites of these zirconium phosphate samples were determined by the method of temperature-programmed desorption (TPD) of ammonia. Helium was used as the carrier gas.

The amount of sample used was between 50 and 200 mg. Ammonia (99.5%) was purified by passing the gas through potassium hydroxide pellets, magnesium sulfate, and finally through a column of 4A molecular sieves. Since the TGA curves (Fig. 1), show no significant loss of material in the range of 200 to 350°C, catalysts were heated at 200°C overnight and then cooled to room temperature (24°C). Ammonia was then injected through a 10-port sampling valve (Valco Instruments Co.) until the catalysts were completely saturated with adsorbed ammonia. The catalysts [except for α-$Zr(HPO_4)_2$ (2.5 : 48)] were then heated at a linear heating rate (2°C/min) in a stream of helium to 100°C, and then maintained at 100°C for 1 h. TPD measurement was completed from 100 to 350°C with a linear heating rate (2°C/min) at a helium carrier gas flow rate of 60 cm³/min (24°C and 1 atm).

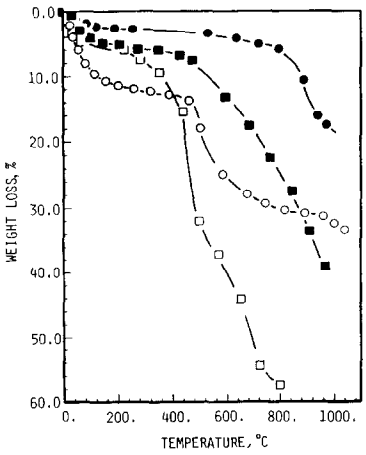


FIG. 1. TG curves of organically pillared zirconium phosphates. (●) P-1-7-7, (■) PP-2-5-12, (○) MPM-6-1, (□) PP-2-5-1.

The procedure for $\alpha$-$Zr(HPO_4)_2$ (2.5 : 48) was similar, except that the desorption of ammonia was operated directly from room temperature to 350°C at a heating rate of 2°C/min. The amount of ammonia desorbed from the catalysts was obtained by integrating the peak area of the TCD response by the method of Simpson's $\frac{3}{8}$ rule.

*Catalytic activity.* The decomposition of isopropyl alcohol was performed in a microcatalytic pulse reactor. Catalyst powder (~100 mg) was packed into a short section of $\frac{3}{8}$-in. stainless-steel (316 SS) tubing. A thermowell was fixed at the center of the catalyst bed to monitor the reaction temperature. Before the inlet of the reactor, the carrier gas (helium, 30 ml/min at 1 atm) was split into two streams; one was passed through the gas 10-port sampling valve and catalyst bed, and the other bypassed the reactor. The bypass stream and that exiting from the reactor were joined and fed into the Poropak S column for analysis of the products by gas chromatography (GC).

Before the reaction, catalysts were preheated overnight at 200°C. Isopropanol was kept in a three-stage saturator and a stream of helium passing through the trap carried saturated isopropanol vapor (vapor pressure of ca. 40 Torr at 24°C) into the loop (3.77 ml) of the 10-port sampling valve. After switching to the injection mode of the sampling valve, the helium saturated with isopropanol in the sampling loop was fed into the reactor. The tubing after the reactor was wound with heating tape and the temperature was kept at 150°C to avoid product condensation in the line.

Apparent residence time, $W/F$, is defined in this paper to be the ratio of catalyst weight ($W$, mg) to flow rate of helium stream ($F$, ml/min) into the reactor. Also, $F$ is defined at reaction temperature and a reactor pressure of 30.2 psia.

The products after the reactor were analyzed by a GowMac gas chromatograph, Series 550. A 6-ft Porapak S column was used for separating the product mixture. The column temperature was controlled manually—5 min at room temperature after the injection of isopropanol, 10 min at 70°C, 5 min at 80°C, and finally 130°C for 10 min.

*Measurements of X-ray diffraction powder pattern and TGA.* X-Ray diffraction powder patterns of the catalysts were taken with a Siefert-Scintag PAD-II diffractometer at 1°C/min with Cu$K\alpha$ radiation (Ni filtered). Weight loss data were obtained with a Cahn electrobalance with TG accessories at a heating rate of 4°C/min.

## RESULTS AND DISCUSSION

### *Catalyst Descriptions*

Analytical and TG data for the catalysts used in this study are shown in Table 1 while the TG curves are given in Fig. 1. Interlayer spacings for the preparations are given in Table 2. These were determined from the (002) reflection of the X-ray pattern which represents the distance between adjacent layers (*5*).

It is seen that the interlayer spacing increases with the size of the pillar. This is also reflected in the water contents. Sample P-1-7-7 has a small interlayer spacing and contains almost no water while the catalysts with larger interlayer distances incorporate more than one mole of water. In addition, sample PP-2-5-1 contained 0.638 mol of the diphosphonic acid used for pillaring. This is shown by the high carbon content and the shape of its TG curve. We note that the total weight loss is inordinantly high for this sample and that a large weight loss (29.8%) begins at a temperature of 280°C

TABLE 2

Surface Area and Catalysts Interlayer Spacing

| Sample | Interlayer spacing (nm) | BET surface surface area ($m^2/g$) |
|---|---|---|
| $\alpha$-ZrP (2.5 : 48) | 0.74 | 33 |
| P-1-7-7 | 0.96 | 8.6 |
| MPM-6-1 | 1.08 | 23 |
| PP-2-5-1 | 1.39 | 102 |
| PP-2-5-12 | 1.39 | 342 |

and ends at about 440°C. This loss is due to unbound diphosphonic acid. When the phosphonic acid is bound as a pillar it does not elute below 400°C. Thus, the weight loss which immediately follows (24.6%) is due to bound phosphonate and to the monohydrogen phosphate group decomposition. We note quite different behavior with sample PP-2-5-12. In this case the organic begins to decompose and elute at about 450°C, with no evidence of trapped organic. The incorporation of diphosphonic acid during preparation appears to occur at high ratios of HF to Zr in the reactant mixture. Additional information relevant to this point will be presented in a subsequent paper (*11*).

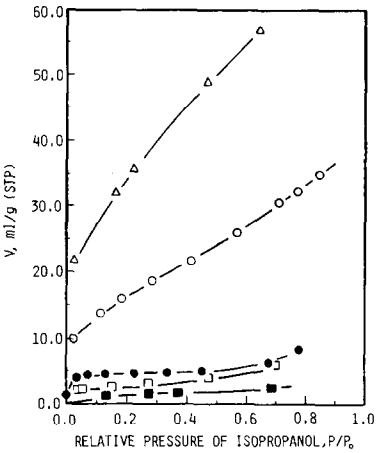


FIG. 3. Isopropanol sorption isotherm at 23°C. (△) PP-2-5-12, (○) PP-2-5-1, (●) α-ZrP (2.5:48), (□) MPM-6-1, and (■) P-1-7-7.

*Surface Areas and Adsorption*

The BET surface areas of the organically pillared zirconium phosphates, shown in Table 2, have been found to increase with the increase in the size of the organic groups in the interlayer. Moreover, PP-2-5-12, which has no trapped diphosphonic acid in the interlayer of the zirconium phosphate, has a BET surface area of 342 $m^2/g$. Thus, the significantly larger surface areas of PP-2-5-1 and PP-2-5-12 suggest that the diphenyl groups have enlarged the intracrystalline pore sizes of zirconium phosphates and the molecules of nitrogen can penetrate into the interlayers. The same order of magnitude of surface areas of phenyl and dimethylphenyl zirconium phosphates as that of α-zirconium phosphate suggests that these two organically pillared compounds have pore window sizes smaller than the size of nitrogen molecules, and only exterior surfaces are available for the BET surface area.

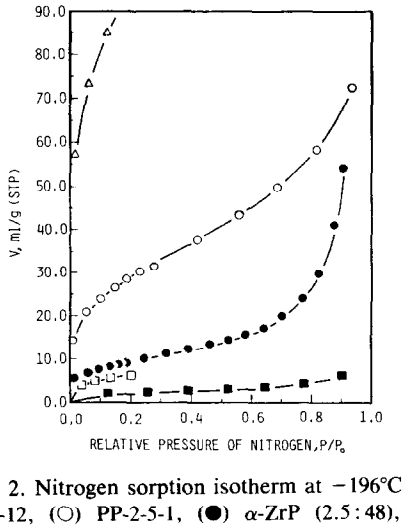


FIG. 2. Nitrogen sorption isotherm at −196°C. (△) PP-2-5-12, (○) PP-2-5-1, (●) α-ZrP (2.5:48), (□) MPM-6-1, and (■) P-1-7-7.

Typical adsorption isotherms for nitrogen and isopropanol are shown in Figs. 2 and 3. These isotherms exhibit the typical Langmuir form for relative pressures up to 0.5. The adsorptive capacity of α-ZrP, MPM-6-1, and P-1-7-7 for isopropanol occurs at relative pressures of less than 0.05, whereas the PP-2-5-1 and PP-2-5-12 continue to adsorb isopropanol at essentially a constant rate up to relative pressures of 0.9 (relative pressure is the pressure divided by the vapor pressure of the adsorbate).

The capacity of the pillared samples for physical adsorption of several adsorbates; isopropanol, 2,2'-dimethyl butane, and perfluorotributylamine; increases with the amount of the nitrogen monolayer or surface area as illustrated in Table 3 (i.e., the adsorptive capacity is PP-2-5-12 > PP-2-5-1

TABLE 3

Monolayer Soption Data

| Adsorbate: | Nitrogen | Water | | Isopropanol | | 2,2'-dimethyl butane | | Perfluorotributyl amine | |
|---|---|---|---|---|---|---|---|---|---|
| Catalyst | g $N_2$ / g catalyst | g $H_2O$ / g catalyst | $\beta$ | g isopropanol / g catalyst | $\beta$ | g 2,2'-dimethyl butane / g catalyst | $\beta$ | g perfluorotributyl amine / g catalyst | $\beta$ |
| $\alpha$-ZrP (2.5:48) | 0.00943 | 0.0107 | — | 0.0111 | — | 0.00472 | — | 0.0167 | — |
| P-1-7-7 | 0.00246 | 0.0108 | 3.86 | 0.00287 | 0.99 | 0.00180 | 1.46 | — | — |
| MPM-6-1 | 0.00524 | 0.0415 | 7.0 | 0.00595 | 0.77 | 0.00233 | 0.89 | — | — |
| PP-2-5-1 | 0.0294 | — | — | 0.0386 | 1.12 | — | — | — | — |
| PP-2-5-12 | 0.0983 | 0.027 | 0.24 | 0.0747 | 0.65 | 0.0664 | 1.35 | 0.189 | 1.08 |

> MPM-6-1 > P-1-7-7). However, the water adsorption on each sample does not follow this trend. MPM-6-1 has a higher capacity for water than the other samples. In contrast to MPM-6-1, PP-2-5-12 has only half the amount of capacity for water adsorption, although it has nearly 20 times the surface area. This indicates that water has penetrated into the interlayers of MPM-6-1. The pore window opening between the layers of MPM-6-1 only allows water molecules or molecules with sizes smaller than water to pass through, since the kinetic diameter of water is 0.265 nm (*12*).

By comparing the monolayer adsorption for $\alpha$-ZrP (2.5:48) with PP-2-5-12, we found that except for water adsorption, PP-2-5-12 always has about a 10-fold increase of monolayer adsorption. This indicates that the molecules with sizes as large as the kinetic diameter of perfluorotributylamine, 1.02 nm (*12*), can penetrate the interlayer space of PP-2-5-12. Furthermore, the relatively smaller amount of monolayer adsorption of water in PP-2-5-12 as compared to the other adsorbates suggests that the diphenyl groups within the interlayers have increased the hydrophobic character of this compound.

In order to compare the relative adsorptive capacity of the pillared catalysts with that of $\alpha$-$Zr(HPO_4)_2$, a new parameter, $\beta$, is introduced in Table 3. $\beta$ is defined as

$$\beta = \frac{W/W_n}{W'/W'_n}$$

where

$W$ = g of adsorbate adsorbed as a monolayer per g of pillared catalyst,

$W_n$ = g of nitrogen adsorbed as a monolayer per g of pillared catalyst,

$W'$ = g of adsorbate adsorbed as a monolayer per g of ZrP (2.5:48),

$W'_n$ = g of nitrogen adsorbed as a monolayer per g of ZrP (2.5:48).

The amount of monolayer is calculated by fitting the BET equation to the adsorption isotherms to determine the monolayer volume of adsorbate. The grams of adsorbate forming a monolayer are calculated by use of the monolayer volume, the molecular weight, and the perfect gas law. The $\beta$ values are based on the assumption that $\alpha$-ZrP (2.5:48) is nonporous, and that all of the adsorbates shown in Table 3 adsorb on the same surface. Therefore, a $\beta$ value of 1 indicates that the adsorbate and $N_2$ adsorb on the same surface whereas a value greater than 1 indicates that the adsorbate has penetrated into more area of the pillared catalyst than nitrogen. The $\beta$ values, shown in Table 3, clearly indicate that water can penetrate into more pores of MPM-6-1 and P-1-7-1 than the nitrogen, since $\beta$ values of 7.00 and 3.06 are obtained. The $\beta$ value also shows the hydrophobic property of PP-2-5-12, since a $\beta$ value of 0.24, which is much smaller than 1, is obtained. The rest of the $\beta$ values for these pillared samples are equal to $1.0 \pm 0.5$.

Since MPM-6-1 and P-1-7-7 have lower

surface areas than α-ZrP (2.5 : 48), while their β values for water are significantly larger than 1, we conclude that these compounds have pore window sizes which allows access to water; however, in their behavior toward the remaining adsorbates, MPM-6-1 and P-1-7-7 are like α-ZrP, which is a nonporous catalyst. If the value for the thickness of the layer, ~0.6 nm, is subtracted from the interlayer spacings, 0.96 nm for P-1-7-7 and 1.08 nm for MPM-6-1, it is recognized that only molecules as small as water, 0.265 nm, can penetrate into the layers. In contrast, PP-2-5-12 was found to have a surface area much larger than α-ZrP (2.5 : 48), and a β value for perfluorotributylamine close to 1. We conclude that water, nitrogen, and perfluorotributylamine all penetrate the interlayers of zirconium phosphates pillared by the diphenyl organic group. The pore window size of this pillared zirconium phosphate is shown to be at least 1.02 nm from the sorption behavior and this accords well with expectations. From the formula (Table 1) we see that roughly half of the phophate positions are pillared. This makes the average interpillar distance 1.06 nm (5) and the free interlayer distance, 0.79 nm.

*Acidic Measurements*

Temperature-programmed ammonia-desorption isotherms are shown in Fig. 4. If it is assumed that the peak at 93°C is from physical adsorption, then five types of sites with different acid strengths may be inferred from changes in the peak shapes between 100 and 386°C for α-ZrP (2.5 : 48). The shapes of the curves for the pillared catalysts are not as distinct as those for the α-ZrP (2.5 : 48). The peaks are broader, and the amount of ammonia desorbed is less than that obtained for α-ZrP (2.5 : 48). This is expected since the pillars replace many of the Brønsted sites. However, two types of acid sites are recognizable. The weaker acid sites are in the range of 100–250°C, and the stronger acid sites cover the range of 250–350°C. Above 350°C, the crystallinity

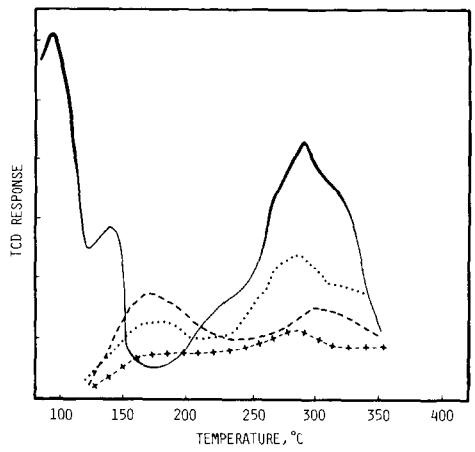


FIG. 4. Temperature-programmed ammonia desorption for zirconium phosphate samples. (—) α-ZrP, (●) P-1-7-7, (– – –) MPM-6-1, (+ – + –) PP-2-5-1. Temperature increasing rate = 2°C/min.

of the sample is lost due to decomposition of the organic. Table 4 shows the amount of ammonia desorbed for these two types of sites. The large number of acidic sites on α-ZrP (2.5 : 48) results from the intercalation of ammonia, which expands the layers and measures the number of internal as well as external sites. The pillared samples desorb less ammonia than α-ZrP (2.5 : 48), but the amount of ammonia desorbed from each pillared sample is the same order of magnitude as shown in Table 4. As shown in Table 4, the number of acidic sites obtained from the experiments from α-ZrP (2.5 : 48), MPM-6-1, and P-1-7-7 are smaller than those calculated from the formula listed in Table 1. The difference is probably due to weak acidic sites where ammonia would be desorbed at temperatures below 100°C. The experimental value for PP-2-5-1 is larger than the expected value. This is probably due to the effect of the trapped diphosphonic acid within PP-2-5-1. Diphosphonic acid should increase the number of acid sites for ammonia chemisorption.

*Catalyst Activity*

Isopropanol decomposition was utilized for the characteriation of the catalyst activities of α-ZrP and the organically pillared

TABLE 4

Acidic Strength Measurement

| Sample | 100–250°C (mmol/g) | 250–350°C (mmol/g) | Total (mmol/g) | Expected[a] |
|---|---|---|---|---|
| α-ZrP (2.5 : 48) | 1.23 | 3.2 | 4.43 | 6.4 |
| PP-2-5-1 | 0.26 | 0.36 | 0.62 | 0.27 |
| MPM-6-1 | 0.49 | 0.51 | 1.00 | 2.37 |
| P-1-7-7 | 0.37 | 0.92 | 1.29 | 2.39 |
| PP-2-5-12 | — | — | — | 1.99 |

[a] Calculations based on the formulas presented in Table 2 with no sorption by the diphosphonic acid.

compounds. The two basic modes of isopropanol decomposition are: (a) dehydration to form propylene and water, and (b) dehydrogenation to form acetone and hydrogen. If propylene is the main product, the catalyst is characterized as an acid type catalyst; if acetone is the main product, the catalyst is characterized as a basic type catalyst (*13*). In our studies of α-ZrP (2.5 : 48) and organically pillared derivatives, propylene and water were the main products from isopropanol decomposition. Only trace amounts of acetone (<1%) were found. Thus, these catalysts can be treated as acid type catalysts.

Reaction of isopropanol at 200°C and 15.5 psig (Table 5), for this series of catalysts, provides the following trend in catalyst activity, PP-2-5-1 > PP-2-5-12 > α-ZrP (2.5 : 48) > P-1-7-7 > MPM-6-1. Nearly 100% selectivity toward propylene and water was obtained for isopropanol decomposition on each catalyst. Only trace amounts disopropyl ether (<1%) were detected in the product stream. No products such as ethylene, butylene, and hexene were found. In contrast to the clean reaction for isopropanol decomposition on zirconium phosphates, propylene, ethylene, and butylene were obtained when using silicalite.

TABLE 5

Kinetic Results of Isopropanol Dehydration

| Catalyst | $k_1$(mg/ml/min) at 200°C | Apparent activation energy (kcal/mol) |
|---|---|---|
| α-ZrP (2.5 : 48) | 0.243 | 21.8 |
| P-1-7-7 | 0.0106 | 18.7 |
| MPM-6-1 | 0.0031 | 21.0 |
| PP-2-5-1 | 2.72 | 12.4 |
| PP-2-5-12 | 1.99 | 14.9 |

Blanton *et al.* (*14*) have shown that for the first-order reaction the kinetic relation between conversion and apparent residence time for pulse reactors are the same as those for steady state reactors. In our studies, the first-order rate expression

$$\log_e \frac{1}{(1-x)} = k\left(\frac{W}{F}\right),$$

where $x$ is the conversion, $W/F$ is proportional to the apparent residence time, and $k$ is the rate constant; was found to adequately fit the data. Figure 5 shows this first-order kinetic fit. Furthermore, a direct comparison of kinetic results from pulse runs and steady state runs was performed on α-ZrP (2.5 : 48). The data from both reactors give similar results. This suggests that a first-order kinetic fit is applicable to quantitatively interpret the data.

The Arrhenius plots are shown in Fig. 6. The slopes of the straight lines yield the values of the apparent activation energies, which are summarized in Table 5. The activation energies of α-ZrP (2.5 : 48), P-1-7-7, and MPM-6-1 are between 18.7 and 21.8 kcal/mol, which are close to the activation energies reported by Hattori (*15*). In his studies, the activation energies, 23.8 ~ 25.2 kcal/mol, were obtained for the zirconium

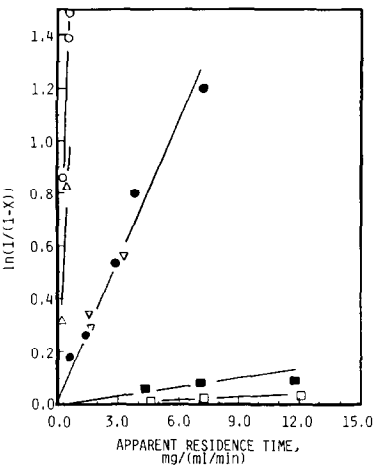


FIG. 5. First-order kinetic fit for isopropanol dehydration at 200°C and 15.5 psig. (○) PP-2-5-1, (△) PP-2-5-12, (▽) α-ZrP (2.5 : 48) (plug flow reactor), (●) α-ZrP (2.5 : 48) (pulse reactor), (■) P-1-7-7, and (□) MPM-6-1.

phosphate pretreated at 300 to 400°C before the reaction. Hattori also found that the activation energies increased to even higher values if the zirconium phosphate was pretreated at higher temperatures. For pretreatment at 800°C, an activation energy of 35.8 kcal/mol was obtained. Clearfield (*16*) reported that zirconium pyrophosphate will be formed by the dehydroxylation of zirconium phosphate at temperatures above 400°C. Thus, the increase of activation energies as the pretreatment temperature is increased probably corresponds to the decomposition of isopropanol over various mixtures of α-ZrP and zirconium pyrophosphate.

The activation energies for isopropanol dehydration on α-ZrP (2.5 : 48), P-1-7-7, and MPM-6-1 are close to those for zeolite Y and X, about 20 kcal/mol, when using a pulse reactor (*17–19*). First-order kinetics were also reported for the zeolites when using the pulse reactor.

The activation energies of PP-2-5-1 and PP-2-5-12, organically pillared diphenyl zirconium phosphate, are significantly lower than those of α-ZrP (2.5 : 48), MPM-6-1, and P-1-7-7. The rate constants based per milligram of catalyst of these two diphenyl pillared zirconium phosphate are significantly larger than those of the other organically pillared catalysts. In the previous section on adsorption studies, we concluded that the pore size of the diphenyl pillared compounds is greater than the size of isopropanol. Therefore, isopropanol molecules can diffuse into the interlayers of this zirconium phosphate catalyst, and the dehydration reaction can occur within the interlayers. Thus, the low activation energies of PP-2-5-1 and PP-2-5-12 suggest a diffusion limitation for the dehydration reaction.

The rate constant for PP-2-5-1 is larger than that for PP-2-5-12 although the surface area of PP-2-5-1 is smaller than that of PP-2-5-12. As has been discussed in the section on catalyst description there is a significant amount of diphosphonic acid trapped inside PP-2-5-1. The trapped diphosphonic acid has apparently increased the catalytic activity of PP-2-5-1.

## CONCLUSIONS

1. Dehydration rather than dehydrogenation is the main reaction of isopropanol over the zirconium phosphate based catalysts. The acid sites are weak since only

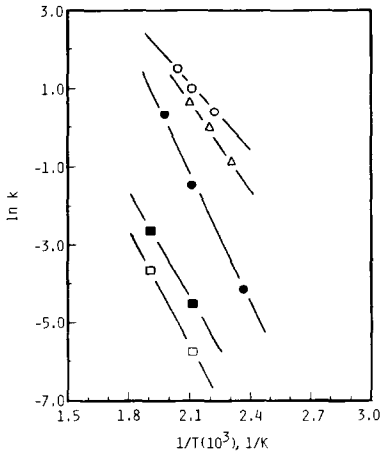


FIG. 6. Arrhenius plot of isopropanol dehydration. (○) PP-2-5-1, (△) PP-2-5-12, (●) α-ZrP (2.5 : 48), (■) P-1-7-7, and (□) MPM-6-1.

dehydration occurred with no secondary reactions.

2. The diphenyl pillared compounds had the highest activity for isopropanol dehydration among the catalysts tested.

3. The adsorption studies illustrated the hydrophobic nature of PP-2-5-12, and that only diphenyl pillared material had pore sizes large enough for penetration of isopropanol into the intracrystalline particle.

4. The reaction appears to occur on the surface of the particles of $\alpha$-ZrP (2.5 : 48) and the compounds pillared by monophenyl or by dimethylphenyl group. However, on the diphenyl pillared derivative, a significant diffusion limitation is suggested by the low activation energy. Hence, the reaction appears to be occurring between the inner layers of this catalyst. Even with this diffusion limitation, the diphenyl pillared compounds are significantly more active than the other catalysts tested.

5. The different bands of temperature-programmed ammonia desorption between $\alpha$-ZrP (2.5 : 48) and organically pillared zirconium phosphate derivatives demonstrate that the strength of acidic sites changes when the organic pillar compounds are inserted between the layers.

## ACKNOWLEDGMENTS

This work was supported by Texaco Inc. and Amoco Chemical Corp. under The Texas A&M Research Foundation Project RF 4911, for which grateful acknowledgment is made.

## REFERENCES

1. Clearfield, A., and Thakur, D. S., *J. Catal.* **54,** 185 (1980).
2. Cheung, H. H.-C., "The Characterization of Catalytic Properties of Copper(II) Exchanged Zirconium Phosphate," Ph.D. thesis. Texas A&M University, College Station, 1982.
3. Cheng, S., and Clearfield, A., *J. Catal.* **94,** 455 (1985).
4. Cheng, S., Peng. G.-Z., and Clearfield, A., *Ind. Eng. Chem. Prod. Res. Dev.* **23,** 219 (1984).
5. Clearfield, A., and Smith, G. D., *Inorg. Chem.* **8,** 431 (1969).
6. Clearfield, A., *in* "Inorganic Ion Exchange Materials" (A. Clearfield, Ed.). CRC Press, Boca Raton, Fla., 1982.
7. Dines, M. B., Giacomo, D. Callahan, P. M., Griffith, K. P., Lane, R. H., and Cooksey, R. E., *in* "Catalytically Modified Surfaces in Catalysis and Electrocatalysis" (J. Miller, Ed.), ACS Symposium Series 192. Amer. Chem. Soc., Washington, D.C., 1982.
8. Clearfield, A., and Berman, J. R., *J. Inorg. Nucl. Chem.* **43,** 2141 (1981).
9. Dines, M. B., and DiGiacomo, P. M., *Inorg. Chem.* **20,** 92 (1981).
10. Dines, M. B., Rieci, E., Griffith, P. C., and Lane, R. H., *Inorg. Chem.* **22,** 1003 (1983).
11. Peng, G.-Z., Yang, M. C.-Y., and Clearfield, A., to be submitted.
12. Breck, D. W., "Zeolite Molecular Sieves." Wiley, New York, 1974.
13. Krylov, O. V., "Catalysis by Nonmetals: Rules for Catalyst Selection." Academic Press, New York, 1970.
14. Blanton, W. A., Jr., Byers, C. H., and Merrill, R. P., *Ind. Eng. Chem. Fundam.* **17,** 4, 611 (1968).
15. Hattori, T., Ishiguro, A., and Murakami, Y., *Nippon Kagaku Kaishi* **6,** 761 (1971).
16. Clearfield, A., Stynes, J. A., *J. Inorg. Nucl. Chem.* **26,** 117 (1964).
17. Stone, F. S., and Agudo, A. L., *Z. Phys. Chem. (Frankfurt)* **64,** 161 (1969).
18. Topchieva, K. V., and Tkhoang, H. S., *Kinet. Catal. (Engl. Transl.)* **14,** 398 (1973).
19. Topchieva, K. V., and Tkhoang, H. S., *Kinet. Catal. (Engl. Transl.)* **14,** 1491 (1973).